JBC RESEARCH ARTICLE

Nicotinamide N-methyltransferase mediates lipofibroblast–myofibroblast transition and apoptosis resistance

Received for publication, November 1, 2022, and in revised form, June 1, 2023 Published, Papers in Press, July 7, 2023,
https://doi.org/10.1016/j.jbc.2023.105027

Mohammad Rehan[1,*], Brian Deskin[1,2], Ashish R. Kurundkar[3], Santosh Yadav[1,2], Yasuka Matsunaga[1], Justin Manges[1,2], Nia Smith[1,2], Kevin G. Dsouza[3], Matthew E. Burow[1], and Victor J. Thannickal[1,2,*]

From the [1]John W. Deming Department of Medicine, Tulane University School of Medicine, New Orleans, Louisiana, USA; [2]Southeast Louisiana Veterans Health Care System, New Orleans, Louisiana, USA; [3]Division of Pulmonary, Allergy, and Critical Care Medicine, Department of Medicine, University of Alabama at Birmingham, Birmingham, Alabama, USA

Reviewed by members of the JBC Editorial Board. Edited by Alex Toker

Metabolism controls cellular phenotype and fate. In this report, we demonstrate that nicotinamide N-methyltransferase (NNMT), a metabolic enzyme that regulates developmental stem cell transitions and tumor progression, is highly expressed in human idiopathic pulmonary fibrosis (IPF) lungs, and is induced by the pro-fibrotic cytokine, transforming growth factor-β1 (TGF-β1) in lung fibroblasts. NNMT silencing reduces the expression of extracellular matrix proteins, both constitutively and in response to TGF-β1. Furthermore, NNMT controls the phenotypic transition from homeostatic, pro-regenerative lipofibroblasts to pro-fibrotic myofibroblasts. This effect of NNMT is mediated, in part, by the downregulation of lipogenic transcription factors, TCF21 and PPARγ, and the induction of a less proliferative but more differentiated myofibroblast phenotype. NNMT confers an apoptosis-resistant phenotype to myofibroblasts that is associated with the downregulation of pro-apoptotic members of the Bcl-2 family, including Bim and PUMA. Together, these studies indicate a critical role for NNMT in the metabolic reprogramming of fibroblasts to a pro-fibrotic and apoptosis-resistant phenotype and support the concept that targeting this enzyme may promote regenerative responses in chronic fibrotic disorders such as IPF.

The homeostatic maintenance of tissue structure and function is dependent on specialized stem cell niches in adult organs (1). These stem cell niches in mammalian tissues/organs almost uniformly consist of epithelial and endothelial stem cells in proximity with niche-supporting fibroblasts (2–4). In the human adult lung, alveolar epithelial stem cells are supported by a unique population of mesenchymal cells referred to as lipofibroblasts (5–7). During injury repair responses, lipofibroblasts may transition into a pathological, pro-fibrotic mesenchymal phenotype known as myofibroblasts (8). Previous studies by our group have shown that myofibroblasts differentiate in response to the pro-fibrotic cytokine, transforming growth factor-β1 (TGF-β1), and acquire an anti-apoptotic phenotype (9, 10). However, although the phenotypic plasticity of this population is well appreciated (11), the mechanisms for this metabolic reprogramming are incompletely understood.

Nicotinamide N-methyltransferase (NNMT) is an enzyme that is highly expressed in the liver and catalyzes the N-methylation of nicotinamide and other pyridine xenobiotic compounds (12). By utilizing the universal methyl donor S-adenosyl-L-methionine (SAM) in this reaction, NNMT functions as a "methyl sink" in many tissues (13). In early development, consumption of SAM by NNMT makes it unavailable for histone methylation, thus altering the epigenetic landscape in human embryonic stem cells (14). NNMT expression is upregulated in many cancers, specifically in cancer aggressiveness or progression (15). In some cancers, NNMT induces resistance to apoptosis *via* the mitochondrial pathway (16) and mediates epithelial–mesenchymal transition (17). This aggressive cancer phenotype may be related to the tumor-supporting role of the stroma (18). Interestingly, fibrosis within the surrounding stroma may not increase the risk of cancer development but may contribute to disease progression (19). The synergistic relationship between fibrosis and cancer development/progression and their potential metabolic underpinnings deserves further study.

In this report, we demonstrate that NNMT is upregulated in human fibrotic disorders, specifically idiopathic pulmonary fibrosis (IPF), and is induced by TGF-β1 in human lung fibroblasts. Our studies indicate that NNMT functions as a critical switch from a homeostatic fibroblast population (lipofibroblasts) to fibrogenic myofibroblasts that acquire an apoptosis-resistant phenotype. NNMT silencing in human lung fibroblasts promotes lipogenic differentiation, abrogates myofibroblast fate commitment in response to TGF-β1, and lowers the threshold for fibroblast apoptosis. Based on the premise that fibrosis resolution involves both myofibroblast-to-lipogenic de-differentiation (20, 21) and myofibroblast apoptosis (22, 23), this study identifies dual/synergistic roles of NNMT in promoting recalcitrant, non-resolving fibrosis.

* For correspondence: Mohammad Rehan, mrehan@tulane.edu; Victor J. Thannickal, vthannickal@tulane.edu.
Present address for Mohammad Rehan: 3330 Hospital Drive Northwest, Snyder Institute of Chronic Diseases, Cumming School of Medicine, University of Calgary, Calgary, Alberta T2N 4M1, Canada.

Results

NNMT expression is upregulated in myofibroblasts of IPF lung tissues and is induced by TGF-β1

IPF is a prototypical progressive fibrotic lung disease that carries high mortality and morbidity (24, 25). We assessed whether NNMT was differentially expressed within stromal cells of human IPF subjects using publicly available databases (IPF Cell Atlas; http://www.ipfcellatlas.com). In multiple datasets from different groups, we found that gene expression of NNMT was upregulated in mesenchymal/stromal cells, an effect that was more pronounced in the myofibroblast population (Fig. 1, *A–D*). We also analyzed the expression levels of NNMT in a transcriptomic dataset of lung tissues from IPF (n = 102) and control (n = 103) (GSE150910) (https://www.ncbi.nlm.nih.gov/geo/query/acc.cgi?acc=GSE150910) (26); higher expression of NNMT in this dataset (Fig. 1*E*) was associated with upregulated gene expression of α-SMA, Col1a1, and FN1 in IPF (Fig. S1, *A–C*). Immunofluorescence staining of control and IPF lung tissues demonstrated higher expression of NNMT that was localized primarily to interstitial stromal cells in IPF lungs (Fig. S1*D*).

To determine if NNMT is spatially expressed within fibroblastic foci of IPF lung tissues, we performed Digital Spatial Profiling (DSP) for RNA on control and IPF lungs by analyzing Regions of Interest (ROIs) defined by the expression of the myofibroblast marker, α-SMA, within morphological structures representing fibroblastic foci (Fig. S1, *E* and *F*). These ROIs confirmed higher expression of canonical pro-fibrotic maker genes, α-SMA, Col1a1, and FN1 (Fig. S1, *G–I*), while also revealing enrichment of NNMT mRNA within these regions of active tissue remodeling (Fig. 1*F*).

TGF-β1 is a pro-fibrotic cytokine that has been implicated in most, if not all, human fibrotic disorders (27). We examined whether the expression of NNMT is altered in response to TGF-β1 stimulation of human lung fibroblasts (IMR-90); TGF-β1 induced a >15-fold upregulation of NNMT mRNA at 24 h by Affymetrix-based transcriptomic analysis (Fig. 1*G*). This was confirmed by real-time PCR in a time-course study that showed peak expression of NNMT mRNA at 16 h after TGF-β1 treatment (Fig. 1*H*). TGF-β1 induced NNMT upregulation at the protein level was sustained up to 48 h (Fig. 1, *I* and *J*); interestingly, under these serum-free conditions, we also detected a slower rate of NNMT induction in untreated cells (Fig. 1, *K* and *L*). Flow cytometry analysis of fibroblasts from control and IPF subjects stained with APC-labelled NNMT and FITC-labelled α-SMA antibodies showed that, at baseline, NNMT co-positivity with α-SMA is significantly higher in IPF patient-derived fibroblasts compared to control, indicating a correlation of NNMT and α-SMA in myofibroblasts (Fig. 1, *M* and *N*). Together, these data support the elevated expression of NNMT in human IPF lung tissues with a preferential increase in the myofibroblast population; furthermore, NNMT is upregulated at both the mRNA and protein levels in a time-dependent manner by TGF-β1.

NNMT promotes extracellular matrix production, suppresses cellular proliferation, and activates pro-fibrotic metabolic pathways in lung fibroblasts

NNMT may serve as a metabolic hub in controlling pro-fibrotic cellular phenotypes (18). We determined the effects of NNMT silencing on extracellular matrix (ECM) production in human lung fibroblasts. Under baseline conditions (*i.e.*, in the absence of TGF-β1 stimulation), NNMT silencing decreased constitutive levels of Col1a1 but paradoxically increased FN in IMR-90 fibroblasts (Fig. 2, *A–D*). Interestingly, we observed an increase in the expression of key metabolic enzymes that mediate anti-fibrotic effects, the NAD+-dependent deacetylase, sirtuin-3 (SIRT3) (28) and ATP citrate lyase (ACLY) (29, 30); both SIRT3 and ACLY were upregulated when NNMT was silenced (Fig. 2, *A*, *E*, and *F*).

A fundamental principle that governs cellular differentiation is the coordinated suppression of proliferation (31, 32). NNMT knockdown significantly upregulated proliferating cell nuclear antigen and Cyclin D1, markers associated with cell cycle progression (Fig. 2, *A*, *G*, and *H*). To confirm these findings in primary IPF lung fibroblasts, we conducted similar NNMT silencing studies with these disease-associated cells. NNMT knockdown, although relatively less efficient in these cells, resulted in a parallel and significant downregulation of the pro-fibrotic markers, Col1a1, and connective tissue growth factor, while ACLY is upregulated (Fig. S2, *A–E*). Together, these data demonstrate that NNMT controls a switch from a less differentiated, proliferative to a more differentiated, pro-fibrotic fibroblast phenotype.

To elucidate whether NNMT regulates TGF-β1-mediated myofibroblast differentiation and pro-fibrotic metabolic reprogramming, we explored effects of TGF-β1 in NNMT silenced/control human lung fibroblasts. RNA-seq analysis of NNMT-deficient fibroblasts showed reduced mRNA levels of TGF-β1-induced ACTA2, Col1a1, and FN1 (Fig. 2, *I–L*). NNMT silencing inhibited α-SMA expression (Fig. 3, *A–C*) and upregulated SIRT3 (Fig. 3, *A* and *D*) under basal conditions and in response to TGF-β1 stimulation when compared to non-targeting siRNA treated cells. In contrast, the effects of NNMT knockdown on ACLY expression were more robustly appreciated in TGF-β1-stimulated cells (Fig. 3, *A* and *E*), while a super-induction of ACLY was observed in NNMT knockdown cells in response to TGF-β1 (Fig. 3, *A* and *E*). In summary, NNMT functions as a critical mediator of pro-fibrotic metabolic reprograming in human lung fibroblasts.

NNMT regulates lipofibroblast–myofibroblast phenotype transition

There is increasing recognition of the plasticity of mesenchymal cell populations, including cells within the alveolar niche (21, 33). The lipofibroblast is thought to be a critical lung-resident population that provides a niche to alveolar epithelial stem cells and maintains lung homeostasis (4). Lipofibroblasts are characterized by high expression of the transcription factors, peroxisome proliferator-activated receptor-gamma (PPARγ) and transcription factor 21 (TCF21)

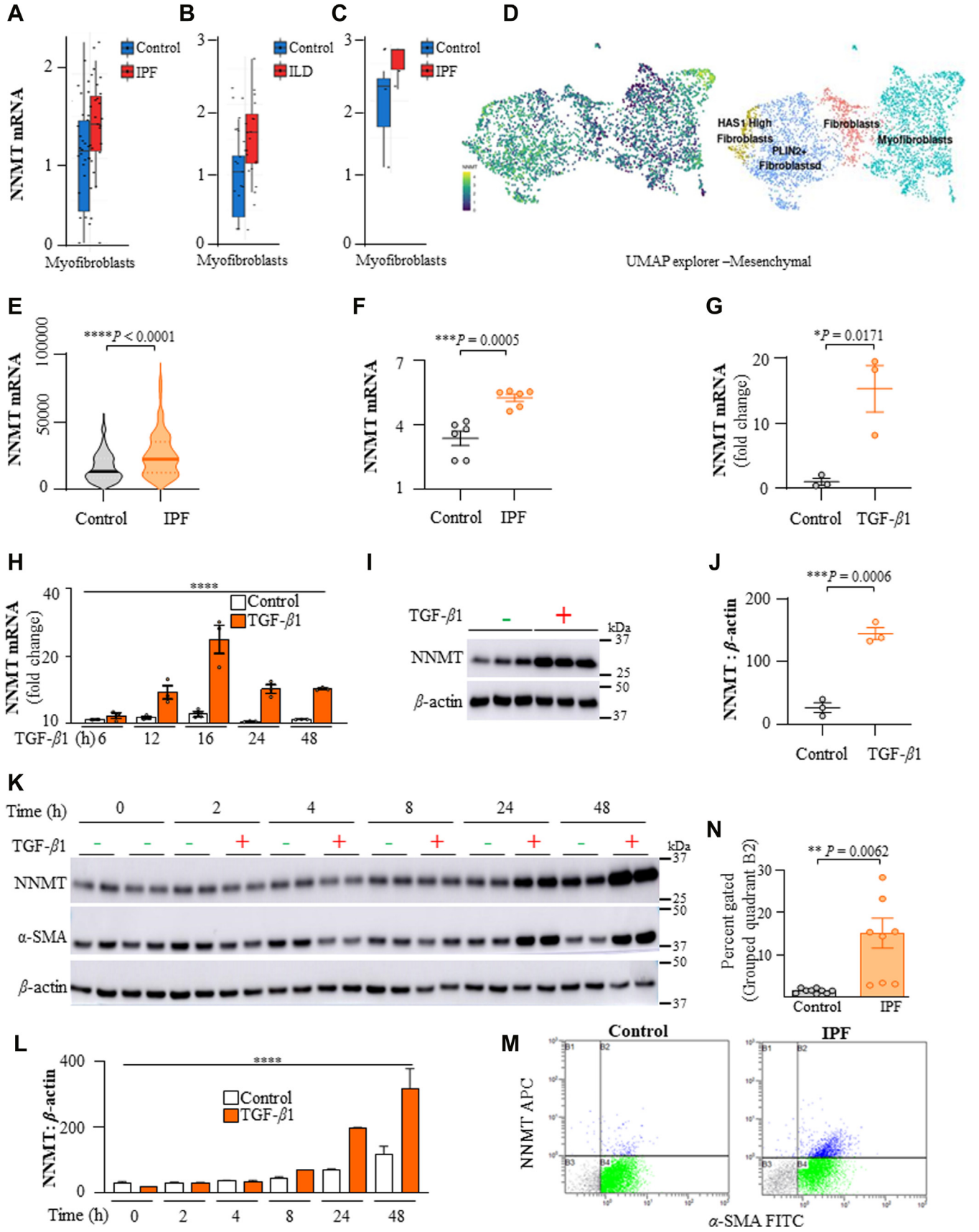

Figure 1. NNMT expression is elevated in myofibroblasts of IPF lung tissues and TGF-β1 stimulated human lung fibroblasts. *A–C*, expression of NNMT transcript in myofibroblasts of control and IPF/ILD lungs in single-cell RNA-seq analysis obtained from different datasets (*A*) Kaminski/Rosas, (*B*) Banovich/Kropski, and (*C*) Lafyatis groups from IPF Cell Atlas. *D*, UMAP plot showing NNMT transcript expression in different mesenchymal cells of control and IPF lungs in single cell RNA-seq analysis obtained from Banovich-Kropski dataset of IPF Cell Atlas. *E*, violin plot showing NNMT mRNA in Gene Expression

(34), and enzymes involved in fatty acid synthesis, transport, and storage: acetyl CoA-carboxylase (ACAC), and Perilin2 (Plin2), respectively. To determine if the transcript levels of these lipofibroblast-associated genes were deficient in IPF, we first queried the publicly available dataset comparing control and IPF lung tissues (GSE150910). Expression levels of lipofibroblast-associated genes were significantly decreased in IPF lung tissues (Fig. 4, *A–D*).

DSP analysis for RNA expression on ROIs of control and IPF lungs showed diminished expression of lipofibroblast specific markers PPARγ in IPF (Fig. S2*F*) while also revealing enrichment of NNMT mRNA within these regions of active tissue remodeling (Fig. 1*G*). These data, along with the data indicating higher levels of myofibroblast markers (Fig. S1, *A–C*), support a potential shift in the lung-resident fibroblast population from a lipofibroblast to myofibroblast phenotype.

Next, we explored whether NNMT may regulate this phenotypic shift. At the mRNA level, TGF-β1 suppressed pro-lipogenic transcription factors, PPARγ and TCF21, while NNMT knockdown mediated the opposite effects (Figs. 2*I* and 4, *E* and *F*); interestingly, although Plin2 mRNA was upregulated by NNMT silencing, this appeared to be further augmented rather than reversed by TGF-β1 (Fig. 4*G*). The effects of TGF-β1 and NNMT silencing on PPARγ and TCF21 were confirmed at protein levels (Fig. 4, *H–K*). The observation that NNMT silencing is insufficient to completely reverse the TGF-β1 effect on this transition raises the possibility of additional NNMT-independent mechanisms by which TGF-β1 suppresses lipogenic differentiation. Flow cytometry analysis of control and IPF patient's fibroblasts stained with APC-labelled NNMT and FITC-labelled PPARγ antibodies showed that, at baseline, NNMT significantly and inversely correlates with PPARγ in patient-derived fibroblasts compared to control, indicating an NNMT mediated negatively regulation of lipogenic differentiation (Fig. 4, *L* and *M*). Together, these data indicate that TGF-β1 and NNMT, independently and coordinately, mediate lipofibroblast-to-myofibroblast phenotypic transition.

NNMT induces apoptosis resistance and mitigates the anti-apoptotic effects of TGF-β1 in lung fibroblasts

Our group and others have shown that TGF-β1 mediates anti-apoptotic effects in lung fibroblasts (10, 35, 36). We sought to determine whether the metabolic and phenotypic shift from lipofibroblasts to myofibroblasts mediated by NNMT is associated with apoptosis resistance and, if so, the specific contribution of NNMT. RNAi-mediated silencing of NNMT appeared to convert the anti-apoptotic effect of TGF-β1 to a pro-apoptotic phenotype, as suggested by light microscopy (Fig. 5, *A* and *B*). We validated this effect of NNMT silencing by monitoring expression levels of activated (cleaved) caspase-3 (Fig. 5, *C* and *D*) and cleaved PARP (Fig. 5, *C* and *E*). Flow cytometry analysis of Annexin V/Propidium iodide staining for apoptosis showed that the TGF-β1 mediated anti-apoptotic effect is completely reversed by NNMT silencing (Figs. 5*F* and S3). To further characterize the effects of NNMT in controlling the apoptosis threshold, we transfected IMR-90 fibroblasts with an NNMT cDNA plasmid and then stimulated cells −/+ TGF-β1. The apoptotic response (measured by Annexin V/Propidium iodide staining and FACS) was suppressed with either NNMT over-expression or TGF-β1; however, the combination did not produce an additive effect (Figs. 5*G* and S4). These data indicate that the apoptosis-resistant phenotype associated with lipofibroblast–myofibroblast transition is largely dependent on NNMT.

NNMT induces the expression of Bcl-2 family member proteins in human lung fibroblasts

Our recent studies support a role for Bcl-2 family proteins in the apoptosis-resistant phenotype of myofibroblasts (28, 37). First, we analyzed the expression levels of pro-apoptotic members of the Bcl-2 family in the existing transcriptomic dataset of IPF lung tissues (GSE150910; IPF, n = 102 and control, n = 103); Bim, Bad, and PUMA were significantly downregulated in IPF lung tissues compared with control (Fig. 6, *A–C*).

We further investigated the mRNA expression levels of pro-apoptotic Bcl-2 family genes in NNMT-silenced fibroblasts treated −/+ TGF-β1. TGF-β1 induced downregulation of Bim and PUMA were completely abrogated by NNMT silencing (Figs. 2*I* and 6, *D* and *E*), and this effect was confirmed at the protein level (Fig. 6, *F–I*). We also confirmed NNMT-mediated regulation of pro-apoptotic proteins in IMR-90 fibroblasts and human IPF lung fibroblasts. NNMT silencing induced higher expression of pro-apoptotic Bcl-2 family proteins, Bim and PUMA, both in IMR-90 and IPF lung fibroblasts (Fig. S5). Together, these data support a critical role for NNMT in mediating anti-apoptotic effects by suppressing the expression of pro-apoptotic Bcl-2 family proteins; and this mediates, at least in part, the anti-apoptotic effects of TGF-β1 in human lung fibroblasts (Fig. 6*J*).

Discussion

Fibroblasts are the primary cells involved in ECM synthesis, deposition, and remodeling in health and disease (20, 38).

Affymetrix data (GSE150910) of control donor and IPF human lungs. Data presented as means ± s.e.m., n = 102 to 103, ****$p < 0.0001$ (Student's *t* test). *F*, mRNA expression of NNMT in Digital Spatial Profiling (DSP) representing six Regions of Interest (ROIs) from control donor and individual with IPF; n = 6, representing one individual. The data are presented as means ± s.e.m., ***$p = 0.0005$ (Student's *t* test). *G*, NNMT mRNA in Gene Expression Microarray of human fibroblasts treated with vehicle or TGF-β1 (2.5 ng/ml) for 24 h. Data presented as means ± s.e.m., n = 3, *$p = 0.0171$ (Student's *t* test). *H*, expression of NNMT mRNA in human fibroblasts treated with or without TGF-β1 (2.5 ng/ml) for indicated time points up to 48 h. Data presented as means ± s.e.m., n = 3, One-way ANOVA. *I* and *J*, Western blot and quantitative analysis of NNMT protein in human fibroblasts treated with TGF-β1 (0 or 2.5 ng/ml) for 48 h. Data presented as means ± s.e.m., n = 3, ***$p = 0.0006$ (Student's *t* test). *K*, Western blot demonstrating expression of NNMT and α-SMA at indicated time points in TGF-β1 (2.5 ng/ml) treatment of human fibroblasts (IMR-90). *L*, quantitative analysis of NNMT protein at indicated timepoints of TGF-β1 treatment from (*K*). Data presented as means ± s.e.m., n = 2, One-way ANOVA. *M*, flow cytometric analysis of control and IPF fibroblasts stained with APC-labelled NNMT and FITC-labelled *α-SMA* is shown. Cells were first gated for FSC and SSC followed by NNMT-APC and *α-SMA*-FITC. *N*, the percentage of cell populations gated in B2 quadrant positive for both NNMT-APC and *α-SMA*-FITC are shown. Results represent data from n = 3 representing fibroblasts of three donor and IPF subjects each. Data presented as means ± s.e.m., n = 3, ***$p = 0.0062$ (Student's *t* test).

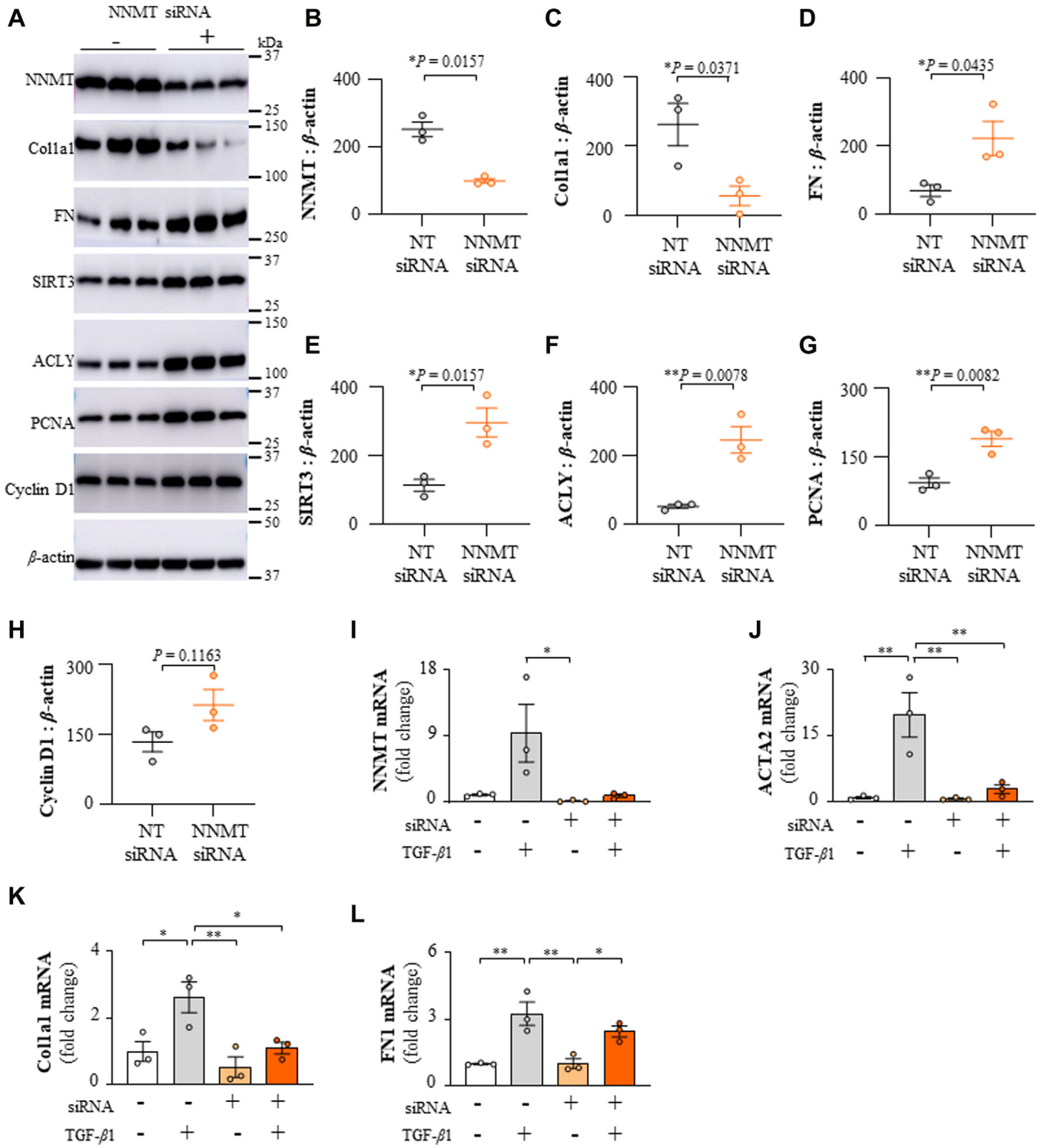

Figure 2. NNMT regulates extracellular matrix production, cellular proliferation, and metabolic pathways in lung fibroblasts. *A–H*, Western blot and quantitative analysis of protein expression of NNMT, Col1a1, FN, SIRT3, ACLY, PCNA, and Cyclin D1 in IMR-90 fibroblasts transfected with non-targeting (NT) or NNMT siRNA (100 nM) for 72 h. Data presented as means ± s.e.m., n = 3, *$p < 0.05$ (Student's *t* test). *I–L*, fold change in mRNAs of NNMT, ACTA2, Col1a1, FN1, and ACLY in RNA-seq analysis of human fibroblasts transfected with non-targeting or NNMT siRNA (100 nM) followed by treatment with TGF-β1 (0 or 2.5 ng/ml) for 48 h. Data presented as means ± s.e.m., n = 3, One-way ANOVA.

Fibroblasts possess remarkable plasticity, and their phenotypic transitions may determine regenerative *versus* fibrogenic responses to lung injury and repair (4, 39). A pathological hallmark of human fibrotic disorders is the persistence of apoptosis-resistant myofibroblasts in injured tissues (23, 25). The persistence and accumulation of these fibrogenic cells have been proposed to be related to either impaired de-differentiation (21, 31, 40) or acquired resistance to apoptosis (36, 41). In this report, we identify a metabolic enzyme that controls both fibroblast phenotype

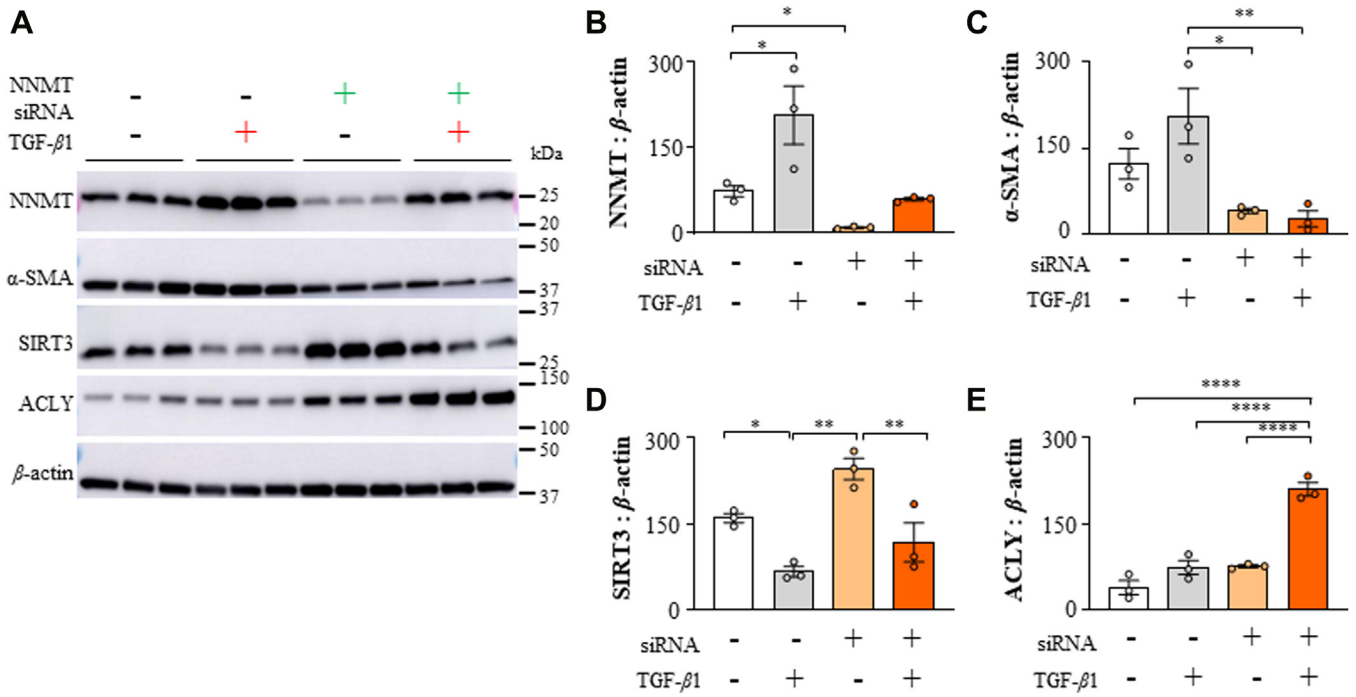

Figure 3. NNMT modulates TGF-β1 induced extracellular matrix production and pro-fibrotic metabolic pathways in human lung fibroblasts. *A–E*, Western blot and quantitative analysis of protein expression of NNMT, α-SMA, SIRT3, and ACLY in human lung fibroblasts transfected with non-targeting or NNMT siRNA (100 nM) followed by treatment with TGF-β1 (0 or 2.5 ng/ml) for 48 h. Data presented as means ± s.e.m., n = 3, One-way ANOVA.

(differentiation > proliferation) and fate (apoptosis resistance > apoptosis susceptibility). Specifically, our studies implicate NNMT as a critical regulator of lipofibroblast-to-myofibroblast transition and apoptosis resistance mediated by altered expression Bcl-2 family proteins (Fig. 6*J*). Importantly, NNMT is highly expressed in fibrotic tissues such as in IPF and in cancers that portend a more aggressive and progressive course, suggesting that this metabolic enzyme may represent a target for therapeutic strategies to retard or even resolve the progressive nature of these morbid conditions.

The importance of metabolic intermediates and bioenergetic states that determine cellular phenotypes and fate is increasingly recognized (42–44). Lipofibroblasts support the alveolar stem cell niche (6, 7), and their presence may be critical to the regenerative capacity of the lung. Previous studies from our group implicated mitochondrial biogenesis, aerobic glycolysis, and glutaminolysis in myofibroblast differentiation, contractility, and apoptosis resistance (11, 45, 46). However, the role of a metabolic enzyme that mediates both myofibroblast differentiation/activation while also suppressing lipogenic differentiation has not, to our knowledge, been previously demonstrated. Our studies clearly demonstrate the NNMT constitutively inhibits TCF21 and PPARγ, master transcription factors of the lipogenic fate of fibroblasts (34). Interestingly, while the anti-diabetic drug, metformin, induces lipogenic differentiation of myofibroblasts to reverse fibrosis (8), it may also restore apoptosis susceptibility to myofibroblasts (47). Whether these dual actions of metformin and NNMT inhibition may function through common metabolic pathways deserves further study, as well as the potential synergy of these interventions.

Our studies demonstrate the coordinate transition of (myo) fibroblasts to a pro-regenerative lipofibroblast phenotype while, at the same time, restoring apoptosis susceptibility when NNMT is silenced; NNMT downregulation also abrogates the anti-apoptotic signaling effects of TGF-β1. This enhanced apoptotic "plasticity" is facilitated by the upregulation of pro-apoptotic Bcl-2 family proteins, Bim and PUMA. Our group recently demonstrated that exogenous delivery of SIRT3, otherwise downregulated in IPF, to the lungs of aged mice alleviates fibrosis by inducing apoptosis in myofibroblasts *via* induction and activation of FoxO3a (28). Apoptosis susceptibility of myofibroblasts is also restored when the H_2O_2-generating enzyme, NADPH oxidase 4 (NOX4), is inhibited (48); the finding that NNMT silencing did not appear to influence NOX4 induction in lung fibroblasts (data not shown) suggests that these TGF-β1 inducible genes may function in parallel pathways to mediate apoptosis resistance.

While our studies support an epigenetic-phenotypic shift from myo- to lipofibroblast differentiation by the induction of TCF21 and PPARγ, further studies are required to interrogate the precise mechanisms for transcriptional regulation when NNMT is silenced. While the predominant effect may be depletion of SAM and histone de-methylation in some tissues (18), in others it may be related to altered bioenergetics such as NAD^+ depletion (49).

The current study presents evidence for a critical role for NNMT in mediating myofibroblast differentiation and apoptosis resistance, hallmarks of the fibrogenic phenotype of tissue-resident fibroblasts. Based on the known homeostatic role of lipofibroblasts in supporting the alveolar epithelial stem cell niche in the lung (6), the potential to modulate fibroblast

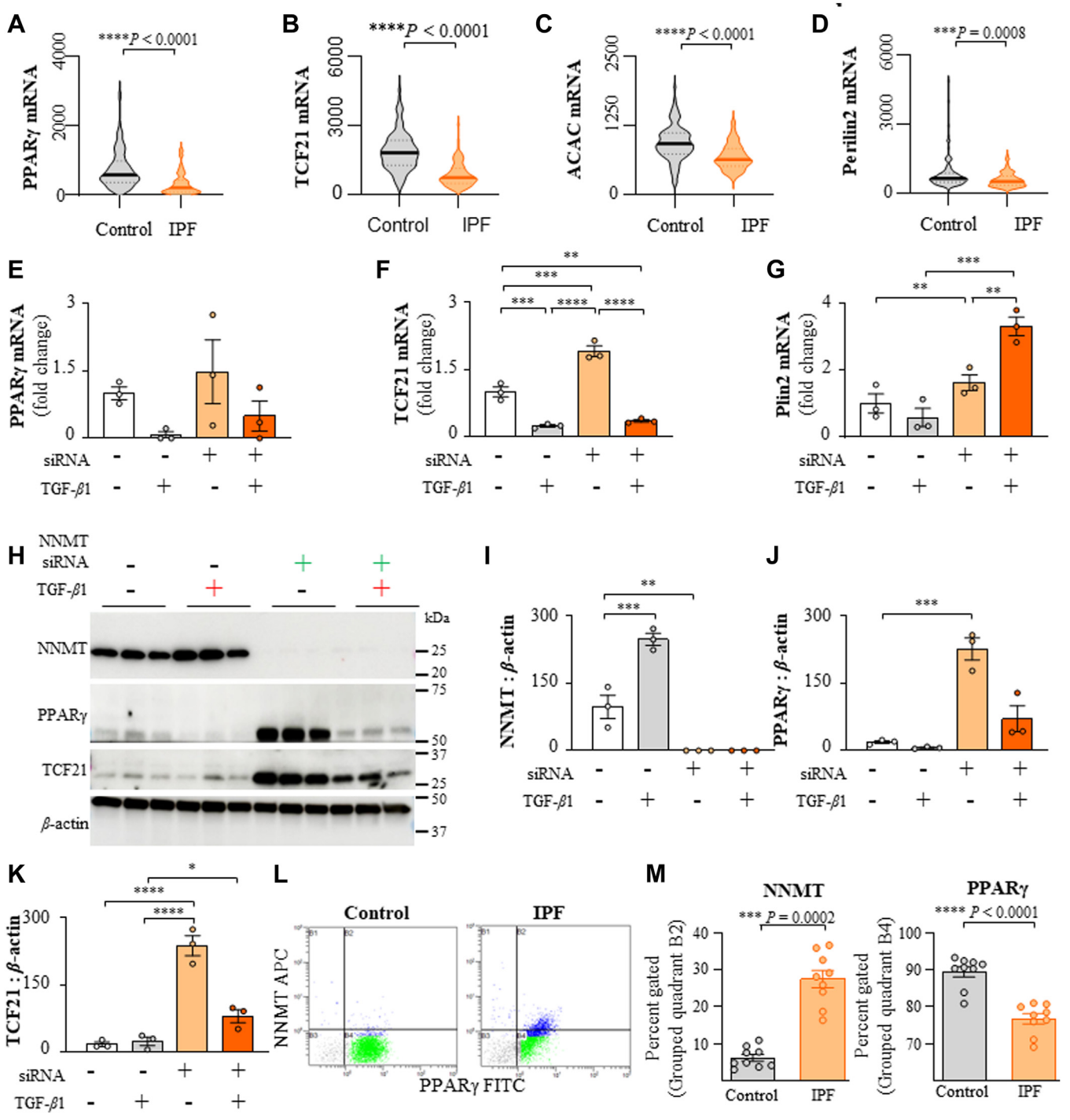

Figure 4. NNMT regulates lipofibroblast-myofibroblast phenotypic transition. *A–D*, violin plots showing mRNA of PPARγ, TCF21, Acetyl-CoA-Carboxylase (ACAC), and Perilin2 in Gene Expression Affymetrix data (GSE150910) of lungs of control donor and IPF patients. Data presented as means ± s.e.m., n = 102 to 103, *$p < 0.005$ (Student's *t* test). *E-G*, mRNA of PPARγ, TCF21, and Perilin2 in RNA-seq analysis of human fibroblasts transfected with non-targeting or NNMT siRNA (100 nM) followed by treatment with TGF-β1 (0 or 2.5 ng/ml) for 48 h. Data presented as means ± s.e.m., n = 3, One-way ANOVA. *H–K*, Western blot and quantitative analysis of NNMT, PPARγ, and TCF21 in whole cell lysates of IMR-90 fibroblasts transfected with NT or NNMT siRNA (100 nM) for 72 h followed by treatment with vehicle or TGF-β1 (2.5 ng/ml) for 36 h. Data presented as means ± s.e.m., n = 3, One-way ANOVA. *L*, flow cytometric analysis of control and IPF fibroblasts stained with APC-labelled NNMT and FITC-labelled PPARγ. Cells were first gated for FSC and SSC followed by NNMT-APC and PPARγ -FITC. *M*, plots show the percentage of population positive for NNMT-APC (grouped quadrant B2) and PPARγ-FITC (grouped quadrant B4) from (*L*). Results represent data from n = 3 representing fibroblasts of three donor and IPF subjects each. Data presented as means ± s.e.m., n = 3, ***$P = <0.0002$ (Student's *t* test).

function from a pro-fibrotic to pro-regenerative phenotype could prove beneficial in progressive fibrotic disorders. Furthermore, our findings are consistent with recent studies supporting NNMT as a master regulator of cancer-associated fibroblasts (18). Thus, therapeutic strategies to downregulate/inhibit NNMT may prove beneficial for progressive diseases

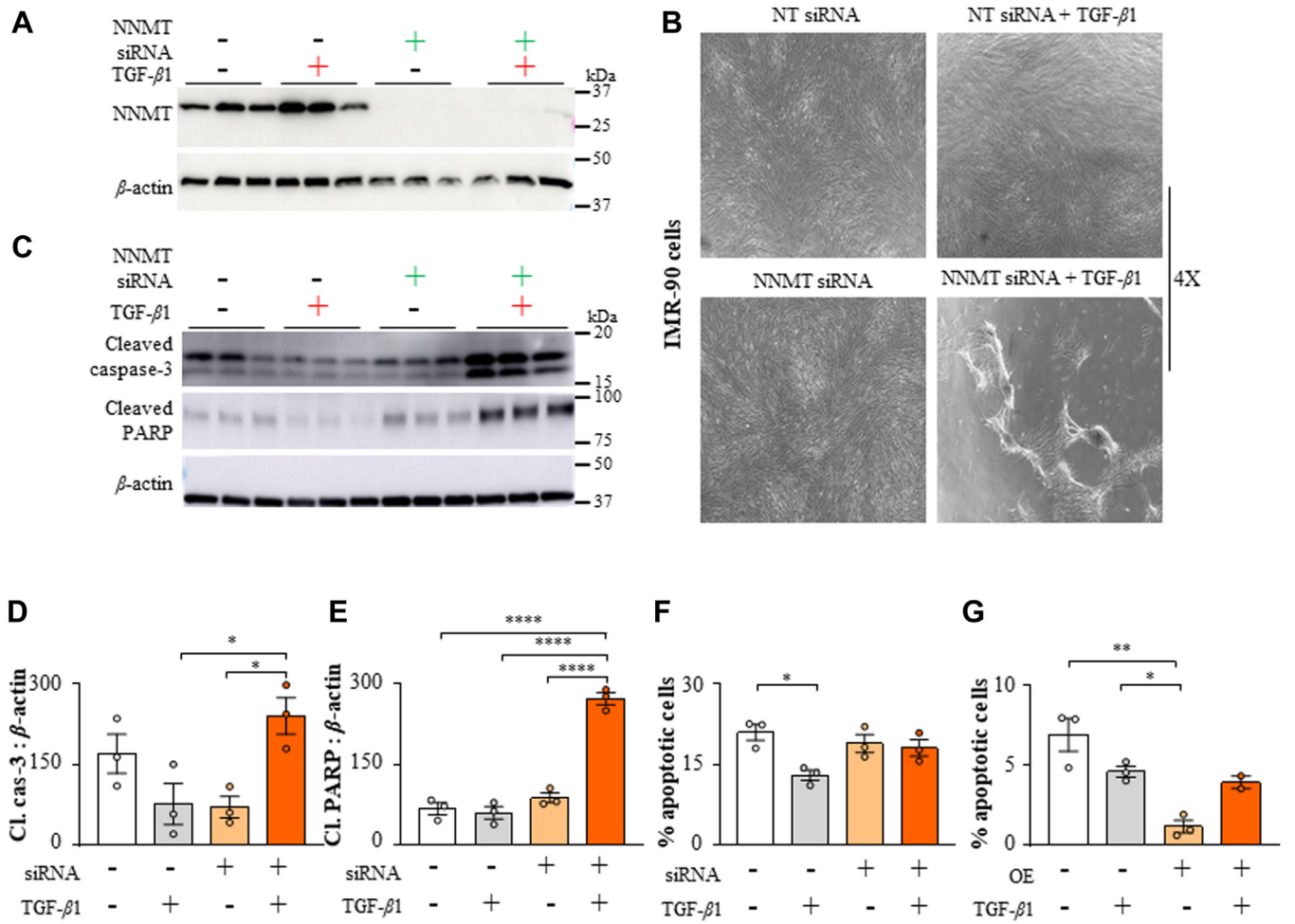

Figure 5. NNMT induces apoptosis resistance and abrogates anti-apoptotic effects of TGF-β1 in lung fibroblasts. *A*, Western blot showing NNMT protein in IMR-90 fibroblasts transfected with NT or NNMT siRNA (100 nM) for 72 h followed by treatment with vehicle or TGF-β1 (2.5 ng/ml) for 36 h. *B*, representative phase contrast images of IMR-90 fibroblasts transfected with NT or NNMT siRNA (100 nM) for 72 h followed by treatment with vehicle or TGF-β1 (2.5 ng/ml) for 36 h. Scale bar 50 μm. *C–E*, Western blot and quantitative analysis of cleaved caspase-3, and cleaved PARP in whole cell lysates of IMR-90 fibroblasts transfected with NT or NNMT siRNA (100 nM) for 72 h followed by treatment with vehicle or TGF-β1 (2.5 ng/ml) for 48 h. Data presented as means ± s.e.m., n = 3, One-way ANOVA. Please note that the β-actin loading control in Figure 5C is the same as shown for Figure 3*A* since the same gel was probed for different proteins (as indicated on the two figures). *F*, quantitation of the apoptotic cells stained with Annexin V and Propidium Iodide after transfection with NT or NNMT siRNA (100 nM) for 72 h followed by treatment with vehicle or TGF-β1 (2.5 ng/ml) for 36 h. Data presented as means ± s.e.m., n = 3, One-way ANOVA. *G*, quantitation of the apoptotic cells stained with Annexin V and Propidium Iodide after transfection with control or NNMT overexpression vector for 48 h followed by treatment with vehicle or TGF-β1 (2.5 ng/ml) for 36 h. Data presented as means ± s.e.m., n = 3, One-way ANOVA.

associated with activated stroma, including progressive fibrotic disorders and aggressive forms of cancer.

Experimental procedures

Reagents

Porcine platelet-derived TGF-β1 was purchased from R&D Systems (Minneapolis, MN, USA). Control (pCMV-3-C-HA, Cat# CV013) and human NNMT over-expressing vectors (pCMV-3-C-NNMT-HA, Cat# HG16767-CY) were purchased from Sino Biological Inc Sources, use and dilutions of antibodies used for the study are provided in Table S1. All kits used in this study have been listed in Table S2.

Human lungs and immunofluorescence staining

The studies of healthy and IPF patient samples were approved by the Tulane University Institutional Review Board. Lung sections were processed and immunofluorescence studies were performed as described previously described (22, 47). Images were acquired using a Nikon A1 laser confocal microscope.

Flow cytometry

To assess percentages of apoptotic cells within individual samples, cells were trypsinized and counted by staining and acquisition as per the manufacturer's instructions (Apoptosis kit, Life Technologies, Catalogue# V13242). For studies involving the co-positivity of NNMT and α-SMA, cells were trypsinized and counted by the trypan blue dye exclusion method. Cells were washed with PBS supplemented with 0.5% BSA followed by incubation with fluorochrome-tagged antibodies at 4 °C for 30 min. The antibody panel was as follows: anti-NNMT-APC (AssayPro, Catalogue# 32655-05161) and anti-α-SMA-FITC (Sigma, Catalogue# F37777) or

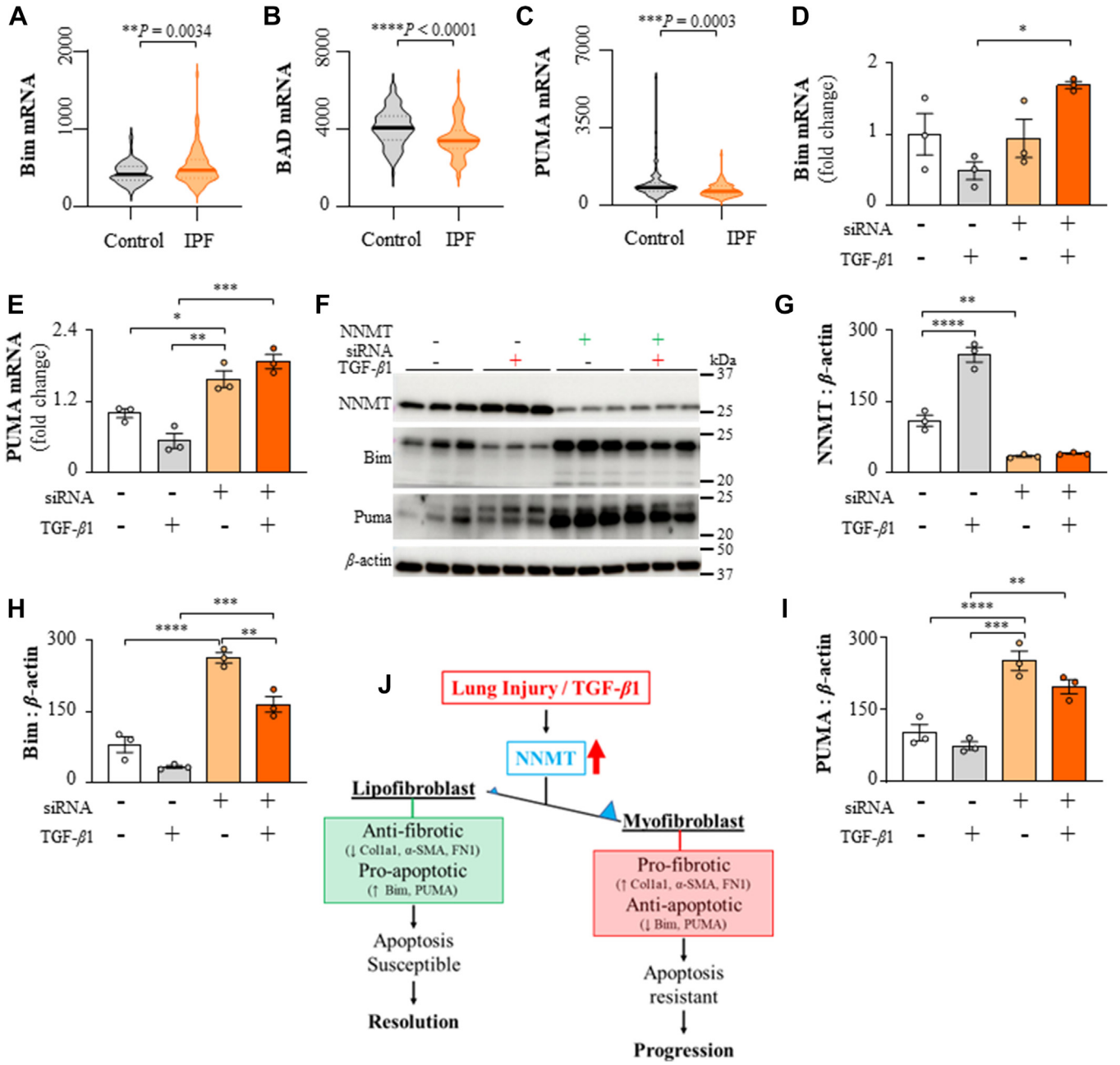

Figure 6. NNMT regulates the expression of Bcl-2 family member proteins in human lung fibroblasts. *A–C*, violin plots showing mRNA of Bim, BAD, and PUMA in Gene Expression Affymetrix data (GSE150910) of lungs of control donor and IPF patients. Data presented as means ± s.e.m., n = 102 to 103, *$p < 0.05$ (Student's *t* test). *D* and *E*, mRNA of Bim and PUMA in RNA-seq analysis of human fibroblasts transfected with non-targeting or NNMT siRNA (100 nM) followed by treatment with TGF-β1 (0 or 2.5 ng/ml) for 48 h. Data presented as means ± s.e.m., n = 3, One-way ANOVA. *F–I*, Western blot and quantitative analysis of expression of NNMT, Bim, and PUMA in whole cell lysates of human donor lung fibroblasts transfected with NT or NNMT siRNA (100 nM) for 72 h followed by treatment with vehicle or TGF-β1 (2.5 ng/ml) for 36 h. Data presented as means ± s.e.m., n = 3, One-way ANOVA. *J*, schematic diagram showing that NNMT regulates lipofibroblast–myofibroblast plasticity and susceptibility to apoptosis.

PPARγ-FITC (Proteintech, Catalogue# CL488-60127). All cells were subsequently washed with PBS/0.5% BSA and resuspended in 1X PBS and acquired on Beckman Coulter Gallios.

Cell culture

Primary lung fibroblasts were isolated and cultured from lung explants of human subjects undergoing lung transplantation with IPF or failed donors (controls), as previously described (48). All studies were approved by the University of Alabama at Birmingham, Birmingham, Alabama, USA. Human fetal lung fibroblasts (Institute of Medical Research; IMR-90) cells were purchased from Coriell Cell Repositories. All cells were cultured as described earlier (50).

Digital Spatial Profiling

The GeoMx Human Whole Transcriptome assay (Nanostring, Inc) was performed to measure mRNA expression levels on formalin-fixed and paraffin-embedded tissues. We

analyzed six Regions of Interest (ROIs) α-SMA positive signals in lung tissue specimens from IPF patients and six ROIs from control lung tissue. This assay was performed on 5 μm slide using a DNA barcoding technology for mRNA detection *via* a UV photocleavable linker. Individual tissue sections were labeled with a cocktail of three fluorescently labeled morphology markers: a Pan-keratin antibody with a green-fluorescent dye, a CD31 antibody with a red fluorescent dye, α-SMA with a yellow-fluorescent dye, and DAPI to detect nuclei. ROIs were selected based on fluorescence imaging. We utilized the commercial service of NanoString Technologies, Inc (2020) for GeoMx Digital Spatial Profiling studies. Normalization of all raw data was done with a negative probe and housekeeper genes.

Western blotting

Cell lysates were prepared in RIPA buffer and Lysates were quantitated using a Micro BCA Protein assay kit (Pierce) according to instructions. Samples were subjected to SDS-PAGE under reducing conditions and western immunoblotting was performed as previously described (22). Densitometric analyses were performed using ImageJ software (http://imagej.nih.gov/ij/).

Real-time PCR and transcriptomic studies

Total RNA from cells was isolated using the RNeasy Mini Kit (Qiagen), and reverse transcribed to cDNA using Bio-Rad iScript cDNA synthesis kit (catalog no. 1708890; Bio-Rad) according to the manufacturer's protocol. Real-time PCR procedure and analysis was performed as described previously Real-time PCR and analysis were performed as described previously (22, 50). Primer sequences used in this study have been provided in Table S3. Transcriptomic studies (Affymetrix U133A chip) on TGF-β1treated IMR-90 cells were as reported previously (GSE17518). RNA-seq processing of NNMT siRNA −/+ TGF-β1 samples were performed and analyzed at Louisiana Cancer Research Center, New Orleans, Louisiana.

RNA interference

Fibroblasts were transfected with 50 to 100 nM targeting or non-targeting siRNA using Lipofectamine-RNaiMAX in Opti-MEM medium (both from Life Technologies), according to the manufacturer's instructions. Briefly, cells (2.5 × 105/well) in 6-well plates were incubated in Opti-MEM medium containing specific or scrambled siRNA (0.1 μM) for 72 h. After incubation with siRNA, the cell culture medium was changed to antibiotic-free DMEM medium supplemented and treated as described in figure legends. The details of NNMT siRNA used in this study have been described in Table S3.

In vitro *overexpression of NNMT*

Cells were grown to 70% confluency and 1 to 2 μg of plasmid were transfected per well of six well plate using FuGENE6 Transfection Reagent (Catalogue Number:E2693) from Promega Corporation, as per manufacturer's instructions. For NNMT overexpression, control (pCMV-3-C-HA-NCV, Sino biological Inc Cat# CV013) or NNMT-HA carrying plasmid (pCMV-3-C-NNMT-HA, Sino biological Inc Cat# HG16767-CY) were used.

TGF-β1 treatment of human fibroblasts

At approximately 70% confluency, fibroblasts were serum starved for 24 h, followed by treatment with 2.5 ng/ml of TGF-β1 in serum-free media for indicated time points.

Statistical analysis and reproducibility

Data are expressed as mean ± s.e.m. Statistical analyses were performed using one-or two-tailed unpaired *t* test or one-way ANOVA to evaluate differences between groups. Analyses were performed using GraphPad Prism software (version 8.4.2), and precise *p*-values are provided. Values of n are provided for each data set with the appropriate statistical methods, representing two or more independent sets of data that showed similar results. Western blot quantification was performed using either ImageQuant TL or ImageJ software (version 1.53a). Graphical drawings were prepared using Adobe Illustrator (version 2020).

Sample sizes

No statistical methods were used to pre-determine sample sizes, but our sample sizes are similar to those reported in previous publications (22, 48, 50).

Data distribution

Data distribution was assumed to be normal, but this was not formally tested.

Blinding

Data collection and analysis were not performed blind to the conditions of the experiment.

Data exclusion

No data exclusions from analyses were made.

Study approval

All experiments were conducted in accordance with approved protocols by Tulane University Institutional Animal Care and Use Committee (IACUC).

Accession code

Microarray data have been deposited in the Gene Expression Omnibus with accession code number GSE17518.

Data availability

The authors declare that the main data supporting the findings of this study are available within the article and its

Supplementary information files. Extra data are available from the corresponding author upon request.

Supporting information—This article contains supporting information (Supplementary Table 1).

Acknowledgments—We wish to sincerely thank Melody C. Baddoo for generous help in RNA-seq data analysis and Alan H. Tucker in FACS experiments.

Author contributions—M. R. and V. J. T. conceptualization; M. R. and V. J. T. methodology; M. R. and B. D. software; M. R. validation; M. R., B. D., A. R. K., S. Y., Y. M., N. S., V. J. T., and M. E. W.: formal analysis; M. R. and B. D. investigation; M. R. and V. J. T. data curation; M. R. writing–original draft; M. R., K. G. D., and V. J. T. visualization; J. M. project administration; V. J. T. supervision; V. J. T. development; V. J. T. methodology; V. J. T. funding acquisition; V. J. T. writing–review & editing.

Funding and additional information—This work was supported by US National Institutes of Health grants, P01 HL114470, R01 HL139617, R01 HL151702, and R01 HL152246; and by the U.S. Department of Veterans Affairs Merit Award, I01BX003056. The content is solely the responsibility of the authors and does not necessarily represent the official views of the National Institutes of Health.

Conflict of interest—The authors declare that they have no known competing financial interests or personal relationships that could have appeared to influence the work reported in this paper.

Abbreviations—The abbreviations used are: ACLY, ATP citrate lyase; DSP, Digital Spatial Profiling; ECM, extracellular matrix; IPF, idiopathic pulmonary fibrosis; NNMT, nicotinamide N-methyltransferase; PPARγ, peroxisome proliferator-activated receptor-gamma; ROI, Regions of Interest; SAM, S-adenosyl-L-methionine; SIRT3, sirtuin-3; TCF21, transcription factor 21; TGF-β1, transforming growth factor-β1.

References

1. Xin, T., Greco, V., and Myung, P. (2016) Hardwiring stem cell communication through tissue structure. *Cell* **164**, 1212–1225
2. Chanda, D., Rehan, M., Smith, S. R., Dsouza, K. G., Wang, Y., Bernard, K., *et al.* (2021) Mesenchymal stromal cell aging impairs the self-organizing capacity of lung alveolar epithelial stem cells. *Elife* **10**, e68049
3. Travaglini, K. J., Nabhan, A. N., Penland, L., Sinha, R., Gillich, A., Sit, R. V., *et al.* (2020) A molecular cell atlas of the human lung from single-cell RNA sequencing. *Nature* **587**, 619–625
4. Gomes, R. N., Manuel, F., and Nascimento, D. S. (2021) The bright side of fibroblasts: molecular signature and regenerative cues in major organs. *NPJ Regen. Med.* **6**, 43
5. Al Alam, D., El Agha, E., Sakurai, R., Kheirollahi, V., Moiseenko, A., Danopoulos, S., *et al.* (2015) Evidence for the involvement of fibroblast growth factor 10 in lipofibroblast formation during embryonic lung development. *Development* **142**, 4139–4150
6. Barkauskas, C. E., Cronce, M. J., Rackley, C. R., Bowie, E. J., Keene, D. R., Stripp, B. R., *et al.* (2013) Type 2 alveolar cells are stem cells in adult lung. *J. Clin. Invest.* **123**, 3025–3036
7. McGowan, S. E., and Torday, J. S. (1997) The pulmonary lipofibroblast (lipid interstitial cell) and its contributions to alveolar development. *Annu. Rev. Physiol.* **59**, 43–62
8. Kheirollahi, V., Wasnick, R. M., Biasin, V., Vazquez-Armendariz, A. I., Chu, X., Moiseenko, A., *et al.* (2019) Metformin induces lipogenic differentiation in myofibroblasts to reverse lung fibrosis. *Nat. Commun.* **10**, 2987
9. Thannickal, V. J., Lee, D. Y., White, E. S., Cui, Z., Larios, J. M., Chacon, R., *et al.* (2003) Myofibroblast differentiation by transforming growth factor-beta1 is dependent on cell adhesion and integrin signaling via focal adhesion kinase. *J. Biol. Chem.* **278**, 12384–12389
10. Horowitz, J. C., Lee, D. Y., Waghray, M., Keshamouni, V. G., Thomas, P. E., Zhang, H., *et al.* (2004) Activation of the pro-survival phosphatidylinositol 3-kinase/AKT pathway by transforming growth factor-beta1 in mesenchymal cells is mediated by p38 MAPK-dependent induction of an autocrine growth factor. *J. Biol. Chem.* **279**, 1359–1367
11. Bernard, K., Logsdon, N. J., Ravi, S., Xie, N., Persons, B. P., Rangarajan, S., *et al.* (2015) Metabolic reprogramming is required for myofibroblast contractility and differentiation. *J. Biol. Chem.* **290**, 25427–25438
12. Aksoy, S., Szumlanski, C. L., and Weinshilboum, R. M. (1994) Human liver nicotinamide N-methyltransferase. cDNA cloning, expression, and biochemical characterization. *J. Biol. Chem.* **269**, 14835–14840
13. Ulanovskaya, O. A., Zuhl, A. M., and Cravatt, B. F. (2013) NNMT promotes epigenetic remodeling in cancer by creating a metabolic methylation sink. *Nat. Chem. Biol.* **9**, 300–306
14. Sperber, H., Mathieu, J., Wang, Y., Ferreccio, A., Hesson, J., Xu, Z., *et al.* (2015) The metabolome regulates the epigenetic landscape during naive-to-primed human embryonic stem cell transition. *Nat. Cell Biol.* **17**, 1523–1535
15. Lu, X. M., and Long, H. (2018) Nicotinamide N-methyltransferase as a potential marker for cancer. *Neoplasma* **65**, 656–663
16. Zhang, J., Wang, Y., Li, G., Yu, H., and Xie, X. (2014) Down-regulation of nicotinamide N-methyltransferase induces apoptosis in human breast cancer cells via the mitochondria-mediated pathway. *PLoS One* **9**, e89202
17. Cui, Y., Zhang, L., Wang, W., Ma, S., Liu, H., Zang, X., *et al.* (2019) Downregulation of nicotinamide N-methyltransferase inhibits migration and epithelial-mesenchymal transition of esophageal squamous cell carcinoma via Wnt/beta-catenin pathway. *Mol. Cell. Biochem.* **460**, 93–103
18. Eckert, M. A., Coscia, F., Chryplewicz, A., Chang, J. W., Hernandez, K. M., Pan, S., *et al.* (2019) Proteomics reveals NNMT as a master metabolic regulator of cancer-associated fibroblasts. *Nature* **569**, 723–728
19. Karampitsakos, T., Spagnolo, P., Mogulkoc, N., Wuyts, W. A., Tomassetti, S., Bendstrup, E., *et al.* (2022) Lung cancer in patients with idiopathic pulmonary fibrosis: a retrospective multicentre study in Europe. *Respirology* **28**, 56–65
20. Plikus, M. V., Wang, X., Sinha, S., Forte, E., Thompson, S. M., Herzog, E. L., *et al.* (2021) Fibroblasts: origins, definitions, and functions in health and disease. *Cell* **184**, 3852–3872
21. El Agha, E., Moiseenko, A., Kheirollahi, V., De Langhe, S., Crnkovic, S., Kwapiszewska, G., *et al.* (2017) Two-way conversion between lipogenic and myogenic fibroblastic phenotypes marks the progression and resolution of lung fibrosis. *Cell Stem Cell* **20**, 261–273.e3
22. Hecker, L., Logsdon, N. J., Kurundkar, D., Kurundkar, A., Bernard, K., Hock, T., *et al.* (2014) Reversal of persistent fibrosis in aging by targeting Nox4-Nrf2 redox imbalance. *Sci. Transl. Med.* **6**, 231ra247
23. Horowitz, J. C., and Thannickal, V. J. (2019) Mechanisms for the resolution of organ fibrosis. *Physiology (Bethesda)* **34**, 43–55
24. Thannickal, V. J., Zhou, Y., Gaggar, A., and Duncan, S. R. (2014) Fibrosis: ultimate and proximate causes. *J. Clin. Invest.* **124**, 4673–4677
25. Thannickal, V. J., Toews, G. B., White, E. S., Lynch, J. P., 3rd, and Martinez, F. J. (2004) Mechanisms of pulmonary fibrosis. *Annu. Rev. Med.* **55**, 395–417
26. Furusawa, H., Cardwell, J. H., Okamoto, T., Walts, A. D., Konigsberg, I. R., Kurche, J. S., *et al.* (2020) Chronic hypersensitivity pneumonitis, an interstitial lung disease with distinct molecular signatures. *Am. J. Respir. Crit. Care Med.* **202**, 1430–1444
27. Meng, X. M., Nikolic-Paterson, D. J., and Lan, H. Y. (2016) TGF-beta: the master regulator of fibrosis. *Nat. Rev. Nephrol.* **12**, 325–338
28. Rehan, M., Kurundkar, D., Kurundkar, A. R., Logsdon, N. J., Smith, S. R., Chanda, D., *et al.* (2021) Restoration of SIRT3 gene expression by airway delivery resolves age-associated persistent lung fibrosis in mice. *Nat. Aging* **1**, 205–217

29. Xiong, J., Kawagishi, H., Yan, Y., Liu, J., Wells, Q. S., Edmunds, L. R., *et al.* (2018) A metabolic basis for endothelial-to-mesenchymal transition. *Mol. Cell* **69**, 689–698.e7
30. Yenilmez, B., Kelly, M., Zhang, G. F., Wetoska, N., Ilkayeva, O. R., Min, K., *et al.* (2022) Paradoxical activation of transcription factor SREBP1c and de novo lipogenesis by hepatocyte-selective ATP-citrate lyase depletion in obese mice. *J. Biol. Chem.* **298**, 102401
31. Hecker, L., Jagirdar, R., Jin, T., and Thannickal, V. J. (2011) Reversible differentiation of myofibroblasts by MyoD. *Exp. Cell Res.* **317**, 1914–1921
32. Ruijtenberg, S., and van den Heuvel, S. (2016) Coordinating cell proliferation and differentiation: antagonism between cell cycle regulators and cell type-specific gene expression. *Cell Cycle* **15**, 196–212
33. Lemos, D. R., and Duffield, J. S. (2018) Tissue-resident mesenchymal stromal cells: implications for tissue-specific antifibrotic therapies. *Sci. Transl. Med.* **10**, eaan5174
34. Park, J., Ivey, M. J., Deana, Y., Riggsbee, K. L., Sorensen, E., Schwabl, V., *et al.* (2019) The Tcf21 lineage constitutes the lung lipofibroblast population. *Am. J. Physiol. Lung Cell. Mol. Physiol.* **316**, L872–L885
35. Vittal, R., Horowitz, J. C., Moore, B. B., Zhang, H., Martinez, F. J., Toews, G. B., *et al.* (2005) Modulation of prosurvival signaling in fibroblasts by a protein kinase inhibitor protects against fibrotic tissue injury. *Am. J. Pathol.* **166**, 367–375
36. Thannickal, V. J., and Horowitz, J. C. (2006) Evolving concepts of apoptosis in idiopathic pulmonary fibrosis. *Proc. Am. Thorac. Soc.* **3**, 350–356
37. Zhou, Y., Huang, X., Hecker, L., Kurundkar, D., Kurundkar, A., Liu, H., *et al.* (2013) Inhibition of mechanosensitive signaling in myofibroblasts ameliorates experimental pulmonary fibrosis. *J. Clin. Invest.* **123**, 1096–1108
38. Kulkarni, T., O'Reilly, P., Antony, V. B., Gaggar, A., and Thannickal, V. J. (2016) Matrix remodeling in pulmonary fibrosis and emphysema. *Am. J. Respir. Cell Mol. Biol.* **54**, 751–760
39. Hinz, B., Phan, S. H., Thannickal, V. J., Prunotto, M., Desmouliere, A., Varga, J., *et al.* (2012) Recent developments in myofibroblast biology: paradigms for connective tissue remodeling. *Am. J. Pathol.* **180**, 1340–1355
40. Kato, K., Logsdon, N. J., Shin, Y. J., Palumbo, S., Knox, A., Irish, J. D., *et al.* (2020) Impaired myofibroblast dedifferentiation contributes to nonresolving fibrosis in aging. *Am. J. Respir. Cell Mol. Biol.* **62**, 633–644
41. Hinz, B., and Lagares, D. (2020) Evasion of apoptosis by myofibroblasts: a hallmark of fibrotic diseases. *Nat. Rev. Rheumatol.* **16**, 11–31
42. Saito, S., Deskin, B., Rehan, M., Yadav, S., Matsunaga, Y., Lasky, J. A., *et al.* (2022) Novel mediators of idiopathic pulmonary fibrosis. *Clin. Sci. (Lond.)* **136**, 1229–1240
43. Schworer, S., Vardhana, S. A., and Thompson, C. B. (2019) Cancer metabolism drives a stromal regenerative response. *Cell Metab.* **29**, 576–591
44. Thannickal, V. J. (2013) Mechanistic links between aging and lung fibrosis. *Biogerontology* **14**, 609–615
45. Bai, L., Bernard, K., Tang, X., Hu, M., Horowitz, J. C., Thannickal, V. J., *et al.* (2019) Glutaminolysis epigenetically regulates antiapoptotic gene expression in idiopathic pulmonary fibrosis fibroblasts. *Am. J. Respir. Cell Mol. Biol.* **60**, 49–57
46. Bernard, K., Logsdon, N. J., Benavides, G. A., Sanders, Y., Zhang, J., Darley-Usmar, V. M., *et al.* (2018) Glutaminolysis is required for transforming growth factor-beta1-induced myofibroblast differentiation and activation. *J. Biol. Chem.* **293**, 1218–1228
47. Rangarajan, S., Bone, N. B., Zmijewska, A. A., Jiang, S., Park, D. W., Bernard, K., *et al.* (2018) Metformin reverses established lung fibrosis in a bleomycin model. *Nat. Med.* **24**, 1121–1127
48. Hecker, L., Vittal, R., Jones, T., Jagirdar, R., Luckhardt, T. R., Horowitz, J. C., *et al.* (2009) NADPH oxidase-4 mediates myofibroblast activation and fibrogenic responses to lung injury. *Nat. Med.* **15**, 1077–1081
49. Komatsu, M., Kanda, T., Urai, H., Kurokochi, A., Kitahama, R., Shigaki, S., *et al.* (2018) NNMT activation can contribute to the development of fatty liver disease by modulating the NAD (+) metabolism. *Sci. Rep.* **8**, 8637
50. Kurundkar, D., Kurundkar, A. R., Bone, N. B., Becker, E. J., Jr., Liu, W., Chacko, B., *et al.* (2019) SIRT3 diminishes inflammation and mitigates endotoxin-induced acute lung injury. *JCI Insight* **4**, e120722